

# Poly(ADP-ribose) polymerase is a mediator of necrotic cell death by ATP depletion

Hyo Chol Ha\* and Solomon H. Snyder\*†‡§

Departments of \*Neuroscience, †Pharmacology and Molecular Sciences, and ‡Psychiatry and Behavioral Sciences, Johns Hopkins University School of Medicine, Baltimore, MD 21205

Contributed by Solomon H. Snyder, October 1, 1999

**Apoptotic and necrotic cell death are well characterized and are influenced by intracellular ATP levels. Poly(ADP-ribose) polymerase (PARP), a nuclear enzyme activated by DNA strand breaks, physiologically participates in DNA repair. Overactivation of PARP after cellular insults can lead to cell death caused by depletion of the enzyme's substrate  $\beta$ -nicotinamide adenine dinucleotide and of ATP. In this study, we have differentially elicited apoptosis or necrosis in mouse fibroblasts. Fibroblasts from PARP-deficient (PARP<sup>-/-</sup>) mice are protected from necrotic cell death and ATP depletion but not from apoptotic death. These findings, together with cell death patterns in PARP<sup>-/-</sup> animals receiving other types of insults, indicate that PARP activation is an active trigger of necrosis, whereas other mechanisms mediate apoptosis.**

**P**oly(ADP-ribose) polymerase (PARP; EC 2.4.2.30) is a nuclear enzyme activated by DNA strand breaks, which transfers 50–200 branched chains of ADP-ribose to a variety of nuclear proteins including PARP itself (1, 2). With moderate amounts of DNA damage, PARP is thought to participate in the DNA repair process (3). However, with excessive activation of PARP, its substrate  $\beta$ -nicotinamide adenine dinucleotide (NAD<sup>+</sup>) is depleted, and, in efforts to resynthesize NAD<sup>+</sup>, ATP is also depleted such that cells may die from energy loss (4–6). A role for PARP overactivation in cell death is indicated by the protection against cell death observed after treatment with PARP inhibitors (7, 8) and the pronounced protection against neuronal ischemia (9, 10), myocardial ischemia (11), and diabetic pancreatic damage (12–14) in mice with targeted deletion of PARP (PARP<sup>-/-</sup>; ref. 15). However, PARP<sup>-/-</sup> mice are not protected against cell death elicited by tumor necrosis factor- $\alpha$  and  $\alpha$ -CD95 ( $\alpha$ -Fas) in hepatocytes (16), and  $\gamma$ -irradiation induced killing of PARP<sup>-/-</sup> mice (17).

Cells can die by energy-dependent apoptosis or by necrosis (18, 19). Because overactivation of PARP depletes ATP, we wondered whether this mode of cell death might be selectively associated with necrosis rather than apoptosis. Accordingly, we have compared cellular models of necrosis and apoptosis. To minimize contaminating variables, we employed a single cell type in which different stimuli can elicit necrosis or apoptosis differentially. We used fibroblasts in which DNA-damaging agents such as *N*-methyl-*N'*-nitro-*N*-nitrosoguanidine (MNNG) and hydrogen peroxide (H<sub>2</sub>O<sub>2</sub>) elicit necrosis at high concentration, whereas activation of Fas leads to apoptosis (16, 20, 21). We show that PARP<sup>-/-</sup> fibroblasts are protected from necrotic but not apoptotic death and that necrosis but not apoptosis is associated with ATP depletion.

## Materials and Methods

**Cell Culture.** Mouse embryonic fibroblasts (MEFs) derived from both wild-type and PARP knockout mice were kindly provided by Z. Q. Wang (Institute of Molecular Pathology, Vienna). MEFs were cultured at 37°C (5% CO<sub>2</sub>) in DMEM supplemented with 10% (vol/vol) FBS, 2 mM L-glutamine, 100 units/ml penicillin, and 100  $\mu$ g/ml streptomycin. MEFs were seeded in 6-well plates at  $\approx$ 70% confluence (exponential phase of growth). Cell numbers were similar for PARP<sup>-/-</sup> and PARP<sup>+/+</sup>

MEFs within a given experiment. MNNG was prepared freshly in DMSO such that the final concentration of the solvent was 0.5% (vol/vol) when added to the culture medium. Hydrogen peroxide was diluted in PBS (pH 7.4) and added to the cells at various concentrations.

**Western Blotting.** MEFs were collected by centrifugation after removal from culture plates with trypsin and dissolved in sample buffer (50  $\mu$ l per 10<sup>6</sup> cells) containing 62.5 mM Tris·HCl (pH 6.8), 6 M urea, 10% (vol/vol) glycerol, 2% (vol/vol) SDS, 5% (vol/vol)  $\beta$ -mercaptoethanol, 1 mM DTT, 0.00125% bromophenol blue with freshly prepared protease inhibitors, 1 mM phenylmethylsulfonyl fluoride, 0.001% aprotinin, and 0.001% leupeptin. After sonication for 30 s and incubation at 65°C for 10 min, the proteins (20  $\mu$ l) were separated by SDS/PAGE on a 4–12% gel and transferred to nitrocellulose membranes (Schleicher & Schuell) for Western blot analyses. The blots were blocked in 5% (vol/vol) nonfat dry milk in PBS-Tween [0.1% (vol/vol) Tween 20] and incubated with PARP antibody at 1:5,000 dilution (SA252, Biomol, Plymouth Meeting, PA), which was based on sequence from the C-terminal portion of the bovine PARP automodification domain (residues 471–493), linked by a multiple antigenic peptide.  $\beta$ -actin (Sigma) was used as a loading control. The Amersham Pharmacia ECL system was used for detection. HL60 cell extracts (SW-101 and SW-102, Biomol) were used as a Western-blotting control to detect intact and cleaved PARP.

**Measurement of ATP.** Intracellular ATP was extracted from cells in the exponential phase of growth and measured by the luciferin/luciferase method by using an ATP Determination Kit (Molecular Probes). The whole cell population, including any floating cells, was subjected to the assay. The reconstituted buffer (200  $\mu$ l) containing 0.5 mM luciferin, 1.25  $\mu$ g/ml luciferase, 25 mM Tricine buffer (pH 7.8), 5 mM MgSO<sub>4</sub>, 100  $\mu$ M EDTA, and 1 mM DTT was mixed with cell lysate (20  $\mu$ l). Luminescence was analyzed after a 2-s delay with a 10-s integration on a Monolight 2010 luminometer (Analytical Luminescence Laboratory, San Diego). A standard curve was generated from known concentrations of ATP in each experiment and used to calculate the concentration of ATP in each sample. Luminescence increased linearly with the ATP concentration in the samples over the range of concentrations measured. The results were normalized by using either cell number or cellular protein as determined by a bicinchoninic acid protein assay (Pierce, Rockford, IL).

Abbreviations: PARP, poly(ADP-ribose) polymerase; NAD<sup>+</sup>,  $\beta$ -nicotinamide adenine dinucleotide; MNNG, *N*-methyl-*N'*-nitro-*N*-nitrosoguanidine; MEFs, mouse embryonic fibroblasts; MTT, 3-(4,5-dimethylthiazol-2-yl)-2,5-diphenyl tetrazolium bromide; DPQ, 3,4-dihydro-5-[4-(1-piperidinyl)butoxyl]-1(2H)-isoquinolinone; CHX, cycloheximide.

§To whom reprint requests should be addressed. E-mail: ssnyder@jhmi.edu.

The publication costs of this article were defrayed in part by page charge payment. This article must therefore be hereby marked "advertisement" in accordance with 18 U.S.C. §1734 solely to indicate this fact.

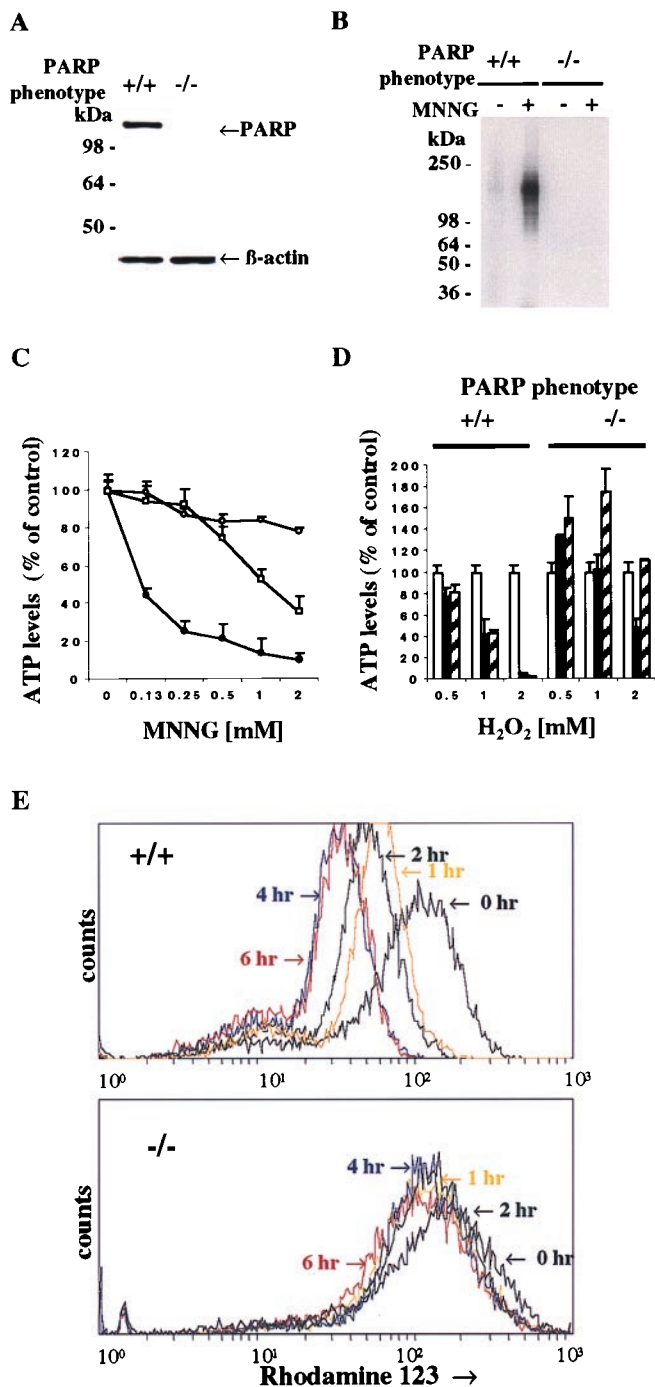


**Fig. 1.** PARP activity regulates intracellular ATP levels. (A) Protein immunoblot analysis of PARP expression in PARP<sup>+/+</sup> and PARP<sup>-/-</sup> MEFs. The PARP<sup>-/-</sup> lane confirms the absence of PARP protein in MEFs of PARP<sup>-/-</sup> mice. Total protein from PARP<sup>+/+</sup> and PARP<sup>-/-</sup> MEFs was separated by SDS/12% PAGE. β-Actin (Sigma) was used as a loading control. (B) Activation of PARP catalytic activity in the PARP<sup>+/+</sup> but not PARP<sup>-/-</sup> MEFs (arrow). Both PARP<sup>+/+</sup> and PARP<sup>-/-</sup> MEFs were treated with 0.5 mM MNNG for 1 hr, and PARP catalytic activity was assayed as described (38). (C) Treatment with MNNG depleted intracellular ATP in wild-type but not PARP<sup>-/-</sup> MEFs. Solid circles, PARP<sup>+/+</sup> MEFs; open circles, PARP<sup>-/-</sup> MEFs; open squares, PARP<sup>+/+</sup> MEFs with 10 μM 3,4-dihydro-5-[4-(1-piperidinyl)butox]-1(2H)-isoquinolinone (DPQ). MNNG depleted intracellular ATP in a concentration-dependent manner. The depletion of intracellular ATP markedly diminished in PARP<sup>-/-</sup> and in PARP<sup>+/+</sup> treated with DPQ. The data are presented as percentage of control content for each of two genotypes. The initial values of ATP level were 3.31 ± 0.36 nmol per 1 × 10<sup>6</sup> cells for PARP<sup>+/+</sup> and 3.50 ± 0.13 nmol per 1 × 10<sup>6</sup> cells for

**Cell Viability and Mitochondrial Membrane Potential Assays.** Cell viability was determined by the mitochondrial-dependent reduction of 3-(4, 5-dimethylthiazol-2-yl)-2,5-diphenyl tetrazolium bromide (MTT) to MTT formazan as described. MTT was added to MEFs to a final concentration of 0.5 mg/ml and incubated for 2 hr. The resulting MTT formazan crystals were dissolved by adding anhydrous isopropanol containing 0.1 N HCl. MTT reduction was determined spectrophotometrically at 570 nm. For measurement of mitochondrial membrane potential, adherent and nonadherent MEFs that were either treated with MNNG or untreated were harvested and incubated in 100 nM rhodamine 123 (Molecular Probes) for 15 min at 37°C as reported (22). Cells were then washed twice, resuspended in PBS, and analyzed on a Becton Dickinson fluorescence-activated cell sorter (FACScan).

**Image Analysis.** The mode of necrotic cell death was determined in part with the combination of two fluorescent dyes, propidium iodide and Hoechst 33342 (Molecular Probes), as described (23). Both dyes stain DNA; however, propidium iodide is membrane impermeant and yields red fluorescent chromatin, whereas Hoechst 33342 is membrane permeant and yields blue pseudo-colored fluorescent chromatin. Necrotic cells have larger nuclei with red fluorescence, whereas viable cells are stained only with green fluorescence. Adherent cells and cells that detached spontaneously were processed separately. Adherent cells were washed in PBS and then stained with Hoechst 33342 (0.1 mg/ml) and propidium iodide (0.1 mg/ml) for 10 min at 37°C. Cells were again washed in PBS and fixed with 3.7% (vol/vol) paraformaldehyde. Exponentially growing MEFs were treated with Fas/cycloheximide (CHX) for 24 hr. Adherent cells were harvested with trypsin and combined with cells floating in the medium. Apoptotic morphology was assayed by Hoechst 33342 staining. MEFs were washed with PBS and fixed with 360 μl of solution containing 0.7% Nonidet P-40, 4.7% (vol/vol) formaldehyde, and 10 μM Hoechst 33342 in PBS.

## Results

**PARP Activity Regulates Intracellular ATP Levels.** In Western blot analysis, PARP protein is absent from the fibroblasts of PARP<sup>-/-</sup> animals (Fig. 1A). Treating the fibroblasts with MNNG, a potent DNA alkylating agent, leads to pronounced activation of PARP catalytic activity reflected in transfer of [<sup>32</sup>P]NAD<sup>+</sup> to PARP protein as ADP-ribose groups (Fig. 1B). Treatment with MNNG for 1 hr depletes ATP from fibroblasts in a concentration-dependent fashion (Fig. 1C). Virtually complete protection against MNNG-induced ATP depletion is evident in PARP<sup>-/-</sup> fibroblasts with substantial protection afforded to wild-type fibroblasts by the PARP inhibitor DPQ.

We also examined H<sub>2</sub>O<sub>2</sub>, which is well known to induce oxidative stress leading to DNA damage (Fig. 1D). H<sub>2</sub>O<sub>2</sub> also depletes ATP from wild-type fibroblasts in a time- and concentration-dependent fashion. PARP<sup>-/-</sup> cells are completely pro-

PARP<sup>-/-</sup>. Intracellular ATP levels were determined by a luciferin/luciferase method. (D) H<sub>2</sub>O<sub>2</sub> depleted ATP levels in wild-type but not PARP<sup>-/-</sup> MEFs. Open bar, 0 hr; solid bar, 1 hr; hatched bar, 2 hr. The H<sub>2</sub>O<sub>2</sub>-induced depletion of intracellular ATP was blocked in PARP<sup>-/-</sup> MEFs. Data are presented as percentage of control content for each of two untreated genotypes. (C–D) Both PARP<sup>+/+</sup> and PARP<sup>-/-</sup> MEFs were treated with various doses of MNNG for 1 hr and H<sub>2</sub>O<sub>2</sub> for 1 and 2 hr. PARP inhibitor, DPQ (10 μM), was pretreated for 3 hr before addition of MNNG. Data are means ± SD of triplicate determinations and representative of at least three experiments. (E) Loss of mitochondrial membrane potential in PARP<sup>+/+</sup> MEFs treated with 5 mM MNNG. PARP<sup>+/+</sup> MEFs lost the mitochondrial membrane potential in a time-dependent manner, whereas PARP<sup>-/-</sup> MEFs showed only slight loss of mitochondrial membrane potential after treatment of MNNG.

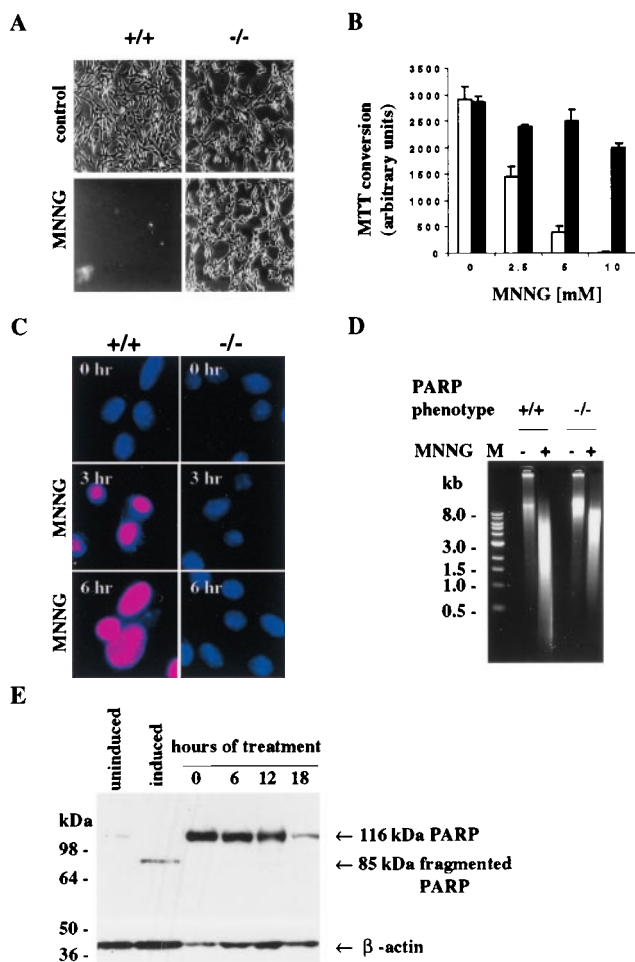


**Fig. 2.** PARP overactivation induced by MNNG mediates necrosis. (A) Morphological profiles of MNNG-induced cell death in PARP<sup>+/+</sup> MEFs. PARP<sup>+/+</sup> MEFs treated with MNNG detached from culture plates, whereas PARP<sup>-/-</sup> MEFs treated with MNNG were protected from detachment and were morphologically similar to untreated MEFs. MEFs after treatment of 5 mM MNNG for 3 hr are shown in phase-contrast pictures. All photographs were taken at  $\times 20$  magnification. (B) Viability of MEFs treated with various concentrations of MNNG. Open bar, PARP<sup>+/+</sup> MEFs; solid bar, PARP<sup>-/-</sup> MEFs. PARP<sup>+/+</sup> MEFs lost cell viability, whereas PARP<sup>-/-</sup> MEFs maintained cell viability. Both PARP<sup>+/+</sup> and PARP<sup>-/-</sup> MEFs were treated with various concentrations of MNNG for 6 hr. Cell viability was determined 6 hr later by formazan production from diphenyltetrazolium salt. Data are means  $\pm$  SD of triplicate determinations and representative of at least three experiments. (C) Necrotic cell death induced by MNNG in PARP<sup>+/+</sup> MEFs. Necrotic PARP<sup>+/+</sup> MEFs had orange-red fluorescence, because propidium iodide gained access to the nucleus. Viable PARP<sup>-/-</sup> MEFs had blue fluorescence, because only membrane-permeable Hoechst 33324 gained access to the nucleus, as in untreated MEFs. Both PARP<sup>+/+</sup> and PARP<sup>-/-</sup> MEFs were loaded with propidium iodide (10  $\mu$ g/ml) and Hoechst 33342 (10  $\mu$ g/ml) after 0, 3, and 6 hr after treatment with 5 mM MNNG. (D) Lack of PARP cleavage in PARP<sup>+/+</sup> MEFs treated with 5 mM MNNG. PARP<sup>+/+</sup> MEFs were treated with 5 mM MNNG for 0, 6, 12, and 18 hr. Total protein from PARP<sup>+/+</sup> MEFs was separated by SDS/4–12% PAGE.  $\beta$ -actin was used as a loading control. M, 1-kilobase DNA marker (39). (E) MNNG-induced necrotic DNA damage. Treatment of MEFs with 5 mM MNNG for 6 hr resulted in a DNA smear.

tected against the effects of 0.5 and 1.0 mM H<sub>2</sub>O<sub>2</sub> at 1 and 2 hr and partially protected against 2.0 mM H<sub>2</sub>O<sub>2</sub> at 1 hr. Interestingly, at 2 hr after 0.5 and 1.0 mM H<sub>2</sub>O<sub>2</sub>, ATP levels in PARP<sup>-/-</sup> fibroblasts are significantly higher than in untreated controls. Depletion of ATP from wild-type fibroblasts is maintained at 4 and 6 hr after 2 mM H<sub>2</sub>O<sub>2</sub>, whereas ATP levels in PARP<sup>-/-</sup>

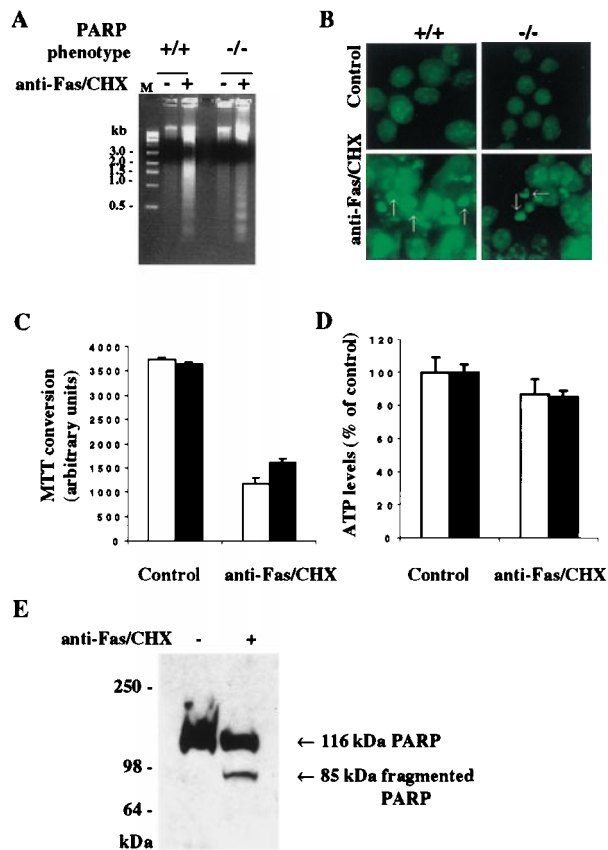


**Fig. 3.** Fas-induced apoptosis without ATP depletion. (A) Fas-induced internucleosomal DNA fragmentation. DNA laddering was essentially the same in PARP<sup>+/+</sup> and PARP<sup>-/-</sup> MEFs treated with anti-Fas and CHX for 24 hr (39). M, 1-kilobase DNA marker. (B) Fas-induced nuclear fragmentation. Nuclear fragmentation (arrows) occurred in both PARP<sup>+/+</sup> and PARP<sup>-/-</sup> MEFs treated with anti-Fas and CHX for 24 hr. After the treatments with anti-Fas and CHX, MEFs were stained with Hoechst 33342. Hoechst 33342-stained apoptotic nuclei had fragmentation with pseudocolored green fluorescence. All photographs were taken at  $\times 20$  magnification. (C) Fas-induced cell death. Open bar, PARP<sup>+/+</sup> MEFs; solid bar, PARP<sup>-/-</sup> MEFs. Both PARP<sup>+/+</sup> and PARP<sup>-/-</sup> MEFs were susceptible to apoptotic cell death induced by anti-Fas and CHX. Cell viability was determined 24 hr later by formazan production from diphenyltetrazolium salt. Data are means  $\pm$  SD of triplicate determinations and representative of at least three experiments. (D) Effects of Fas on intracellular ATP levels. Intracellular ATP levels were maintained in both PARP<sup>+/+</sup> and PARP<sup>-/-</sup> MEFs treated with anti-Fas and CHX. Open bar, PARP<sup>+/+</sup> MEFs; solid bar, PARP<sup>-/-</sup> MEFs. The data are presented as percentage of control content for each of two genotypes. The intracellular ATP levels were determined by a luciferase/luciferase method. (E) Fas-induced cleavage of PARP in PARP<sup>+/+</sup> MEFs. Total proteins from treated and untreated PARP<sup>+/+</sup> MEFs were separated by SDS/4–12% PAGE. (A–E) Both PARP<sup>+/+</sup> and PARP<sup>-/-</sup> MEFs were treated with anti-Fas (100 ng/ml) and CHX (10  $\mu$ g/ml) for 24 hr.

fibroblasts are increased to 160–170% of wild-type control values (data not shown).

Mitochondrial membrane potential assessed with rhodamine 123 is also greatly diminished in wild-type fibroblasts and protected in PARP<sup>-/-</sup> preparations treated with 5 mM MNNG for various time points (Fig. 1E). Hence, overactivation of PARP leads to the loss of mitochondrial membrane potential.

**Overactivation of PARP Induced by MNNG Mediates Necrosis.** Wild-type fibroblasts are killed by the treatment with MNNG as is evident by their detachment from culture plates (Fig. 2A). By contrast, PARP<sup>-/-</sup> fibroblasts are completely protected with morphology resembling that of wild-type cells. As another index

**Table 1. PARP deletion differentiates necrosis and apoptosis**

Tissue	Insults	Pathophysiology	Refs.
Necrosis associated: PARP <sup>-/-</sup> protects			
<i>In vivo</i> models			
	MCAo	Cerebral ischemia	9, 10
	STZ	Diabetic damage	12–14
	Zymosan	Inflammation of multiple organs	32
	LAD-IR	Myocardial ischemia	11
	TNBS	Inflammation of colon	31
<i>In vitro</i> models			
Cerebellum	NMDA, SNP, SIN-1, OGD	Necrosis	9
Thymocytes	ONOO <sup>-</sup> , H <sub>2</sub> O <sub>2</sub>	Necrosis	40
Islet cells	X/XO	Necrosis	41
Apoptosis: PARP <sup>-/-</sup> does not protect			
<i>In vitro</i> models			
Cerebellum	Low K <sup>+</sup> , STA, MPP <sup>+</sup> , ONOO <sup>-</sup> , Colchicine	Apoptosis	16
Thymocytes	Etoposide, DEX, Ceramide, Ionomycin	Apoptosis	16
Hepatocytes	$\alpha$ -CD95, ActD + TNF	Apoptosis	16
Bone marrow	MNU, CPT-11, -IL-3	Apoptosis	42
Splenocytes	MNU	Apoptosis	17
Fibroblasts	$\alpha$ -CD95 + CHX, MMS	Apoptosis	42

MCAo, middle cerebral artery occlusion; NMDA, *N*-methyl-D-aspartate; SNP, sodium nitroprusside; SIN-1, 3-morpholino-sydnimine hydrochloride; OGD, oxygen-glucose deprivation; STA, staurosporine; X/XO, hypoxanthine/xanthine oxidase; TNBS, trinitrobenzenesulfonic acid; STZ, streptozocin; MPP<sup>+</sup>, 1-methyl-4-phenylpyridinium; DEX, dexamethasone; ActD, actinomycin D; MNU, methylnitrosourea; CPT-11, a semisynthetic camptothecin derivative; MMS, *N*-methylmethanesulfonate; TNF, tumor necrosis factor; LAD-IR, ischemia and reperfusion of the left anterior descending coronary artery.

of cell viability, we monitored the conversion of MTT to MTT formazan (Fig. 2B). MNNG markedly reduces this conversion in wild-type cells, consistent with loss of viability, whereas PARP<sup>-/-</sup> fibroblasts are protected. MNNG seems to kill fibroblasts by necrosis.

Plasma membrane integrity is maintained in apoptosis but lost in necrosis (24–27). We stained fibroblasts with two DNA-binding dyes, propidium iodide, which is colored red and does not penetrate intact cell membranes, and Hoechst 33342, which is colored blue and readily penetrates cell membranes (Fig. 2C). In wild-type cells treated with MNNG, nuclei stain intensely for propidium iodide, consistent with a necrotic process. By contrast, nuclei from PARP<sup>-/-</sup> fibroblasts do not stain for propidium iodide but only for Hoechst 33342, consistent with their protection from necrosis. At the 3 and 6 hr times used for the propidium iodide experiments and with the 2.5–10 mM concentration of MNNG employed, ATP levels are fully depleted in wild-type fibroblasts but completely protected in PARP<sup>-/-</sup> cells (data not shown).

MNNG induces necrotic cell death without PARP cleavage (Fig. 2D), which is typically associated with apoptotic cell death (28). Also, MNNG induces DNA smear, which is typically associated with necrosis, in wild-type fibroblasts and, to a lesser extent, in PARP<sup>-/-</sup> fibroblasts (Fig. 2E), indicating that DNA damage is still occurring in the absence of cell death in PARP<sup>-/-</sup> fibroblasts. The absence of PARP cleavage and internucleosomal DNA fragmentation indicates that caspases are not activated in MNNG-induced necrotic cell death.

**Fas Induces Apoptosis Without ATP Depletion.** To evaluate apoptosis, we used Fas, also known as  $\alpha$ -CD95. Fas is a membrane protein that triggers apoptotic cell death when activated by anti-Fas antibodies in conjunction with CHX. In wild-type fibroblasts, Fas activation elicits DNA laddering, which is typically associated with apoptosis (Fig. 3A). Internucleosomal DNA fragmentation in PARP<sup>-/-</sup> fibroblasts is essentially the same as in wild type. Apoptosis is also characterized by membrane-bound nuclear fragments (24–27). Fas activation elicits nuclear fragmentation to a similar extent in wild-type and PARP<sup>-/-</sup> fibroblasts (Fig. 3B).

Fas activation also decreases MTT conversion, indicating both a loss of cell viability and mitochondrial respiration, to a similar extent in wild-type and PARP<sup>-/-</sup> fibroblasts (Fig. 3C). Unlike the necrotic process associated with MNNG or H<sub>2</sub>O<sub>2</sub> treatment, Fas activation does not deplete ATP with no differences between wild-type and PARP<sup>-/-</sup> fibroblasts (Fig. 3D). In apoptotic cell death, PARP is typically cleaved (28). We observe PARP cleavage in Fas-activated fibroblasts but not in MNNG-treated cells, consistent with Fas activation reflecting apoptosis and MNNG treatment involving necrosis (Fig. 3E).

## Discussion

Apoptosis is an active process requiring energy, whereas necrosis has been considered as a passive process. In the present study, we have shown that DNA-damage-induced PARP overactivation depletes intracellular ATP levels irreversibly and induces necrotic cell death, whereas, in PARP<sup>-/-</sup> cells, intracellular ATP levels are maintained without necrotic cell death. On the other hand, after Fas stimulation, both PARP<sup>+/+</sup> and PARP<sup>-/-</sup> fibroblasts maintain intracellular ATP levels and are equally susceptible to apoptosis. Thus, PARP activation seems to regulate the mode of cell death by influencing intracellular ATP levels. This conclusion is consistent with other evidence that depletion of ATP can transform an ongoing apoptotic process into necrosis, suggesting that intracellular ATP levels regulate the mode of cell death (29, 30).

Our findings that PARP deletion protects against necrotic but not apoptotic cell death can explain discrepant results previously reported on the role of PARP in cell death (Table 1). Thus, PARP deletion protects against neurotoxicity caused by activation of glutamate *N*-methyl-D-aspartate receptors (9, 10), myocardial ischemia (11), inflammation elicited by zymosan, bacterial lipopolysaccharide plus interferon- $\gamma$ , and trinitrobenzenesulfonic acid (31–33), as well as streptozotocin-induced diabetes (12–14). In all of these models, abundant evidence indicates that cell death occurs by a necrotic process (24–27). PARP deletion fails to protect against tumor necrosis factor- $\alpha$  and CD95-induced death of hepatocytes (16) as well as death of thymocytes elicited by agents such as ceramide, dexamethasone, etoposide, or ionomycin (16). These forms of cell death are well charac-

terized as apoptotic (16). Furthermore, it has been reported recently that PARP inhibitors block necrotic cell death, but not apoptosis, in Burkitt's lymphoma (34), endothelial (35), and epithelial cells (36). In these studies, PARP inhibitors reverse the mode of cell death from necrosis to apoptosis. These findings, together with results reported here, show a consistent link between PARP and necrosis and the absence of a relationship between PARP and apoptosis.

In apoptosis, PARP protein is typically cleaved and inactivated, which may preserve cellular ATP by preventing its depletion through excessive PARP activation. Preservation of ATP by PARP cleavage thus affords the energy required for apoptosis. This model is supported by a recent report showing that expression of caspase-resistant PARP in fibroblasts transforms apoptosis to necrosis associated with depletion of NAD<sup>+</sup> and ATP (37). PARP's abundance and very high catalytic activity presumably enable its excess activation to mediate this switching of the mode of cell death.

We directly show that PARP activation is required for necrotic cell death, suggesting that this enzyme activation may be regarded as an "active" key link in necrotic cell death. Moreover, because inhibition of PARP activity or PARP gene deletion can inhibit both depletion of ATP and induction of necrosis, PARP

overactivation induced-necrosis is an active process rather than a passive one. In many clinical instances, such as inflammation, vascular stroke, and myocardial infarction, necrosis seems to be the predominant mode of cell death. Accordingly, drugs that inhibit PARP might be expected to be therapeutic. In animal models, PARP inhibition by drugs or gene deletion diminishes tissue damage associated with stroke and myocardial infarct (9–11).

We thank Franck Polleux and Anirvan Ghosh for the morphological study, Jim Flook for expert technical assistance with fluorescence-activated cell-sorting analysis, Akira Sawa for anti-Fas antibody, and Jie Zhang for DPQ. This work was supported by U.S. Public Health Service Grant DA00266 (to S.H.S.) and Research Scientist Award DA00074 (to S.H.S.). Under an agreement between the Johns Hopkins University and Guilford, S.H.S. is entitled to a share of the royalties from sales related to PARP received by Johns Hopkins University from Guilford. The University owns stock in Guilford, with S.H.S. having an interest in the University Share under University policy. S.H.S. serves on the Board of Directors and the Scientific Advisory Board of Guilford. He is a consultant to the company, and he owns additional equity in Guilford. This arrangement is being managed by the University in accordance with its conflict-of-interest policies.

- Lautier, D., Lagueux, J., Thibodeau, J., Menard, L. & Poirier, G. G. (1993) *Mol. Cell. Biochem.* **122**, 171–193.
- de Murcia, G., Schreiber, V., Molinete, M., Saulier, B., Poch, O., Masson, M., Niedergang, C. & Menissier de Murcia, J. (1994) *Mol. Cell. Biochem.* **138**, 15–24.
- Satoh, M. S. & Lindahl, T. (1992) *Nature (London)* **356**, 356–358.
- Berger, N. A. (1985) *Radiat. Res.* **101**, 4–15.
- Carson, D. A., Seto, S., Wasson, D. B. & Carrera, C. J. (1986) *Exp. Cell Res.* **164**, 273–281.
- Oleinick, N. L. & Evans, H. H. (1985) *Radiat. Res.* **101**, 29–46.
- Szabo, C. & Dawson, V. L. (1998) *Trends Pharmacol. Sci.* **19**, 287–298.
- Pieper, A. A., Verma, A., Zhang, J. & Snyder, S. H. (1999) *Trends Pharmacol. Sci.* **20**, 171–181.
- Eliasson, M. J., Sampei, K., Mandir, A. S., Hurn, P. D., Traystman, R. J., Bao, J., Pieper, A., Wang, Z. Q., Dawson, T. M., Snyder, S. H., *et al.* (1997) *Nat. Med.* **3**, 1089–1095.
- Endres, M., Wang, Z. Q., Namura, S., Waeber, C. & Moskowitz, M. A. (1997) *J. Cereb. Blood Flow Metab.* **17**, 1143–1151.
- Zingarelli, B., Salzman, A. L. & Szabo, C. (1998) *Circ. Res.* **83**, 85–94.
- Masutani, M., Suzuki, H., Kamada, N., Watanabe, M., Ueda, O., Nozaki, T., Jishage, K., Watanabe, T., Sugimoto, T., Nakagama, H., *et al.* (1999) *Proc. Natl. Acad. Sci. USA* **96**, 2301–2304.
- Burkart, V., Wang, Z. Q., Radons, J., Heller, B., Herceg, Z., Stingl, L., Wagner, E. F. & Kolb, H. (1999) *Nat. Med.* **5**, 314–319.
- Pieper, A. A., Brat, D. J., Krug, D. K., Watkins, C. C., Gupta, A., Blackshaw, S., Verma, A., Wang, Z. Q. & Snyder, S. H. (1999) *Proc. Natl. Acad. Sci. USA* **96**, 3059–3064.
- Wang, Z. Q., Auer, B., Stingl, L., Berghammer, H., Haidacher, D., Schweiger, M. & Wagner, E. F. (1995) *Genes Dev.* **9**, 509–520.
- Leist, M., Single, B., Kunstle, G., Volbracht, C., Hentze, H. & Nicotera, P. (1997) *Biochem. Biophys. Res. Commun.* **233**, 518–522.
- de Murcia, J. M., Niedergang, C., Trucco, C., Ricoul, M., Dutrillaux, B., Mark, M., Oliver, F. J., Masson, M., Dierich, A., LeMeur, M., *et al.* (1997) *Proc. Natl. Acad. Sci. USA* **94**, 7303–7307.
- Nicotera, P., Leist, M. & Manzo, L. (1999) *Trends Pharmacol. Sci.* **20**, 46–51.
- Leist, M. & Nicotera, P. (1997) *Biochem. Biophys. Res. Commun.* **236**, 1–9.
- Nagata, S. & Golstein, P. (1995) *Science* **267**, 1449–1456.
- Simbulan-Rosenthal, C. M., Rosenthal, D. S., Iyer, S., Boulares, A. H. & Smulson, M. E. (1998) *J. Biol. Chem.* **273**, 13703–13712.
- Vander Heiden, M. G., Chandel, N. S., Williamson, E. K., Schumacker, P. T. & Thompson, C. B. (1997) *Cell* **91**, 627–637.
- Lieberthal, W., Menza, S. A. & Levine, J. S. (1998) *Am. J. Physiol.* **274**, F315–F327.
- Ankarcrona, M., Dypbukt, J. M., Bonfoco, E., Zhivotovsky, B., Orrenius, S., Lipton, S. A. & Nicotera, P. (1995) *Neuron* **15**, 961–973.
- Nicotera, P., Ankarcrona, M., Bonfoco, E., Orrenius, S. & Lipton, S. A. (1997) *Adv. Neurol.* **72**, 95–101.
- Kerr, J. F., Wyllie, A. H. & Currie, A. R. (1972) *Br. J. Cancer* **26**, 239–257.
- Wyllie, A. H., Kerr, J. F. & Currie, A. R. (1980) *Int. Rev. Cytol.* **68**, 251–306.
- Kaufmann, S. H., Desnoyers, S., Ottaviano, Y., Davidson, N. E. & Poirier, G. G. (1993) *Cancer Res.* **53**, 3976–3985.
- Leist, M., Single, B., Castoldi, A. F., Kuhle, S. & Nicotera, P. (1997) *J. Exp. Med.* **185**, 1481–1486.
- Eguchi, Y., Shimizu, S. & Tsujimoto, Y. (1997) *Cancer Res.* **57**, 1835–1840.
- Zingarelli, B., Szabo, C. & Salzman, A. L. (1999) *Gastroenterology* **116**, 335–345.
- Szabo, C., Lim, L. H., Cuzzocrea, S., Getting, S. J., Zingarelli, B., Flower, R. J., Salzman, A. L. & Perretti, M. (1997) *J. Exp. Med.* **186**, 1041–1049.
- Oliver, F. J., Menissier-de Murcia, J., Nacci, C., Decker, P., Andriantsitohaina, R., Muller, S., de la Rubia, G., Stoclet, J. C. & de Murcia, G. (1999) *EMBO J.* **18**, 4446–4454.
- Lee, Y. J. & Shacter, E. (1999) *J. Biol. Chem.* **274**, 19792–19798.
- Walisser, J. A. & Thies, R. L. (1999) *Exp. Cell Res.* **251**, 401–413.
- Filipovic, D. M., Meng, X. & Reeves, W. B. (1999) *Am. J. Physiol.* **277**, F428–F436.
- Herceg, Z. & Wang, Z. Q. (1999) *Mol. Cell. Biol.* **19**, 5124–5133.
- Zhang, J., Dawson, V. L., Dawson, T. M. & Snyder, S. H. (1994) *Science* **263**, 687–689.
- Eldadah, B. A., Yakovlev, A. G. & Faden, A. I. (1996) *Nucleic Acids Res.* **24**, 4092–4093.
- Virag, L., Scott, G. S., Cuzzocrea, S., Marmar, D., Salzman, A. L. & Szabo, C. (1998) *Immunology* **94**, 345–355.
- Heller, B., Wang, Z. Q., Wagner, E. F., Radons, J., Burkle, A., Fehsel, K., Burkart, V. & Kolb, H. (1995) *J. Biol. Chem.* **270**, 11176–11180.
- Oliver, F. J., de la Rubia, G., Rolli, V., Ruiz-Ruiz, M. C., de Murcia, G. & Murcia, J. M. (1998) *J. Biol. Chem.* **273**, 33533–33539.